

## Supplementary Materials: Riverine nitrogen flux and its response to management, climate, and other environmental factors in Northeast and Midwest United States

Nicolas Eduardo Maxfield and Richard A. Smith

### Regional Description

In the NE, 50% of TN flux originates from human sources primarily in cities and suburbs (see Figure S1). Meanwhile, in the MW, 46% of TN flux comes from crops and livestock, representing the combined application of nitrogen fertilizer, manure, and biological fixation (see Figure S1). In both regions, atmospheric deposition is a major contributor (approximately 30%). Additionally, the NE and MW offer unique hydrological and meteorological environments. In the NE, modelled TN flux is transported to 250 points along the Atlantic coast, with nearly 50% being delivered at the mouths of the Susquehanna, Delaware, Hudson, Potomac, and Connecticut Rivers. All of the rivers in the NE have an average length and drainage area of 56 km and 1,601 km<sup>2</sup> respectively. In the MW, on the other hand, the region can be divided into three major rivers, the Missouri, Ohio, and Upper Mississippi Rivers, all of which drain into the same terminal point of the lower Mississippi River at the intersection of the Missouri, Arkansas, and Tennessee state boundaries. These have a mean length of 2,706 km and the entire drainage area (2.3 million km<sup>2</sup>) drains into the same point.

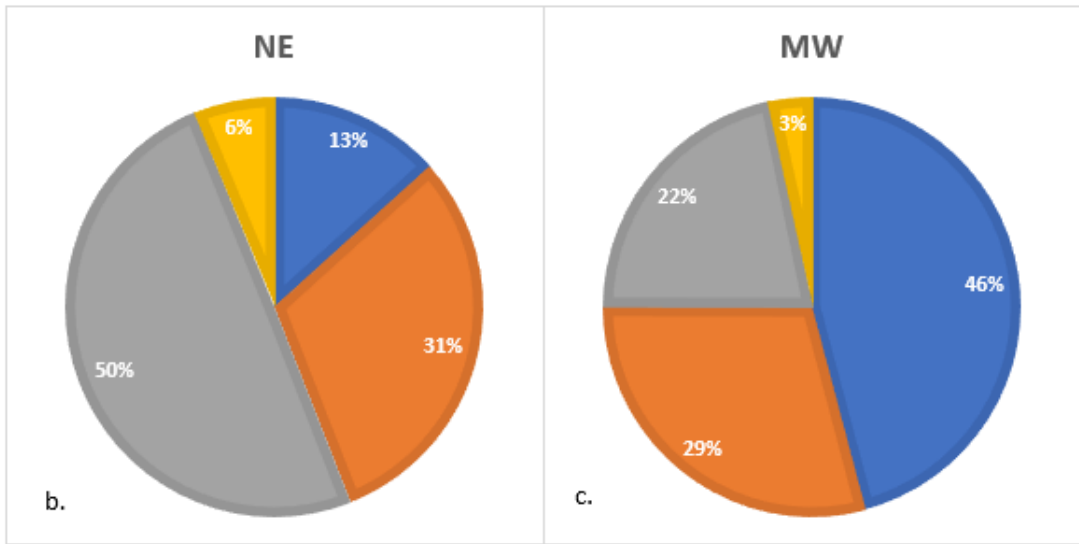
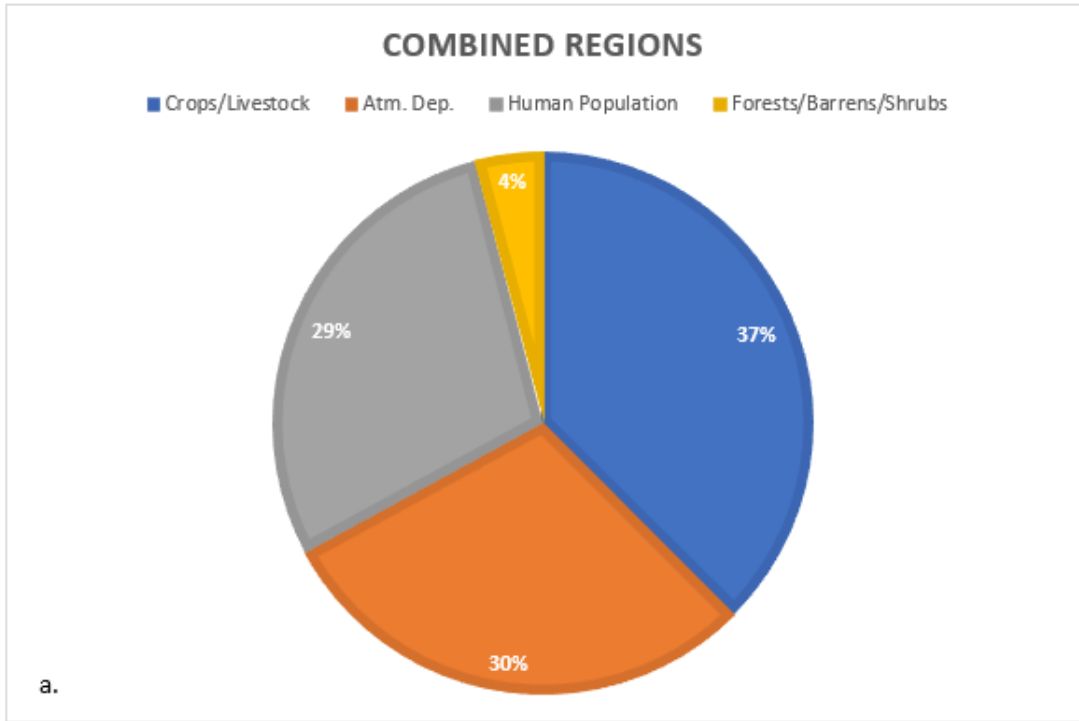


Figure S1 shows the fraction of TN delivered to receiving waters from each major nitrogen source. Figure S1.a. shows the fractions from the Northeast (NE) and Midwest (MW) combined. Figure S1.b. shows the sources of TN flux from the NE delivered to 250 coastal points along the Atlantic coast. Figure S1.c. shows the sources of TN flux from the MW delivered to the lower Mississippi River at the intersection of the Missouri, Arkansas, and Tennessee state boundaries.

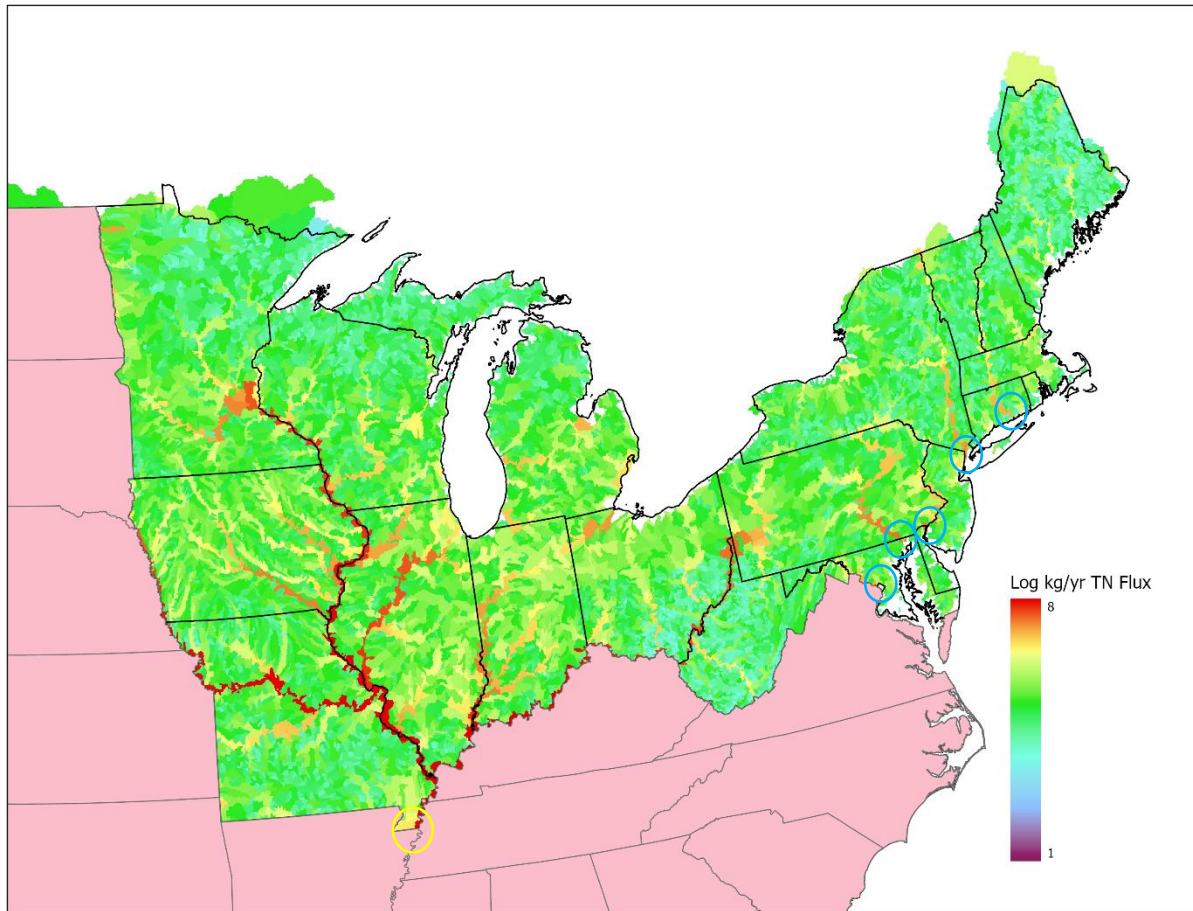


Figure S2 shows the  $\log_{10}$  of  $\text{kg N yr}^{-1}$  at each RF1 catchment in the regions. The yellow circle shows the downstream point to which all of the MW's TN flux passes to the Lower Mississippi River. The blue circles show where nearly 50% of TN flux enters the Atlantic Coast.

## SPARROW Model Recalibration

Statistical calibration of SPARROW models has the simultaneous goals of optimizing the overall model accuracy and assessing the relative importance of the individual explanatory watershed factors and statistical significance. The model is calibrated to represent steady-state conditions for the continental United States, meaning that the factors reflect mean annual conditions over the period of 1985-1994 (Smith, et al., 1997). The model uses nitrogen source inputs (population, atmospheric deposition, crop nitrogen/manure application/biological fixation, and land extent of crop and natural lands). Land-to-water factors processing of these inputs are soil permeability, temperature, precipitation, stream density, cropland drainage, and the frequency of extreme dry/wet/hot/cold (Alexander, et al., 2008; Shih, et al., 2022; Maxfield, et al., 2021). In-stream processing is determined by water time-of-travel and reservoir hydraulic load (see Equation S1; for a complete list of model parameters and model regression output, see Table S1).

Equation S2

$$FLUX_i = \left\{ \sum_{j \in J(i)} \left[ \sum_{n=i}^N S_{n,j} \beta_n \exp(-\alpha' Z_j) \right] \prod_m \exp(-\delta_m^s T_{i,j,m}) \prod_l 1/(1 + \lambda^r q_{i,j,l}^{-1}) \right\} \exp(\varepsilon_i)$$

Where FLUX is the monitored TN flux at the mouth of each stream reach  $i$ . For the sources delivered from land to water, from point sources to water, and from upstream reaches  $j$ ,  $S_n$  is the source input from source *type*  $n$ ;  $\beta$  is the coefficient assigned to that source;  $\alpha$  is the associated coefficient for a given land characteristic  $Z_j$  for reach watershed  $j$ . For factors associated with aquatic transport,  $\delta^s$  is the associated coefficient for a given river transport time  $T$  for each reach mouth  $m$ ; and  $\lambda^r$  is the reservoir rate coefficient for a given hydraulic load  $q$ . Finally,  $\varepsilon$  is the statistical error term.

In regards to climate, the original SPARROW model had precipitation and temperature. Because SPARROW relies on long-term climate conditions that would not reflect the occurrence of sub-annual climate extremes, we developed four climate extreme frequency land-to-water transport factors (wet month frequency, dry month frequency, hot month frequency, and cold month frequency). These were developed using the standardized precipitation index (SPI) (McKee, et al., 1993) for wet/dry and standardized temperature index (STI) (Burke, et al., 2017) for hot/cold extremes.

Table S3 shows the regression results for the SPARROW recalibration, and Table S4 shows the overall measures of model fit. Dry (1.24<sup>1</sup>/3.85<sup>2</sup>), hot (-0.96/-2.32), and cold (1.26/2.91) month frequency are statistically significant. Meanwhile wet month frequency (0.31/0.70) is not statistically significant. The modeled TN flux has an R-squared value of 0.94.

---

<sup>1</sup> Coefficient estimate

<sup>2</sup> t-value

Table S3 shows the regression coefficients and measures of statistical fit for the current SPARROW nitrogen flux model

Parameter	Units	Estimate	Std Err	t Value	Pr >  t	VIF (NC)
Population	kg N/person/year	2.690	0.325	8.287	0.000	1.614
Atmospheric Deposition	dimensionless	0.802	0.170	4.731	0.000	7.021
Corn and Soy	dimensionless	0.150	0.025	5.974	0.000	3.534
Alfalfa	dimensionless	0.088	0.058	1.512	0.131	3.500
Wheat	dimensionless	0.125	0.056	2.253	0.025	1.687
Other crops	dimensionless	0.065	0.029	2.239	0.026	4.803
Unrecovered Animal Waste	dimensionless	0.057	0.054	1.062	0.289	7.455
Forest	kg N/km <sup>2</sup> /year	103.651	36.783	2.818	0.005	4.722
Barren	kg N/km <sup>2</sup> /year	351.896	270.410	1.301	0.194	2.014
Shrub	kg N/km <sup>2</sup> /year	120.845	53.648	2.253	0.025	2.547
Tiles	percent	0.008	0.003	2.337	0.020	2.503
Permeability	log(cm/hr)	-0.122	0.049	-2.517	0.012	1.670
Temperature	°C	-0.054	0.011	-5.043	0.000	3.328
Precipitation	cm	0.012	0.002	7.699	0.000	4.543
Specific catchment area	log(m)	0.532	0.163	3.269	0.001	1.796
Drainage density	log(km <sup>-1</sup> )	0.248	0.106	2.350	0.019	3.914
Wet month frequency	count SPI > 2	0.314	0.452	0.695	0.487	1.238
Dry month frequency	count SPI < -2	1.236	0.321	3.851	0.000	2.038
Hot month frequency	count STI > 2	-0.955	0.412	-2.319	0.021	2.673
Cold month frequency	count STI < -2	1.255	0.431	2.908	0.004	1.466
River mass transport	m/year	0.052	0.008	6.598	0.000	5.800
Reservoir transport	m/year	1.380	0.592	2.330	0.020	1.482

Table S4 shows statistical measures of fit for the current SPARROW TN flux model

N Obs	DF Model	DF Error	SSE	MSE	Root MSE	R-Square	Adj R-Sq	Yld R-Sq
425	22	403	116	0.288	0.537	0.937	0.934	0.875

## Model Simulation

Model simulation required dynamical inputs of each source, land-to-water delivery factor, and aquatic decay factor. Each decadal timestep (1980s, 1990s, 2000s, and 2010s) represents mean annual conditions (e.g. mean annual temperature for 1980-1989 is used as the temperature input for 1980s). Prior to use in the model, inputs are adjusted to the SPARROW calibration data. Table S3 provides a description and the data source for each simulated factor.

Table S3 shows the data used for simulating TN flux.

Name	Description	Citation
Population	Number of people	(CIESIN, 2018)
Wastewater Treatment	Portion of nitrogen removed from influent at each wastewater treatment facility.	(Skinner & Maupin, 2012; Rychtecka, et al., 2010)
Land Use/Cover	Extent of cropland, natural land, and developed land	(Kicklighter, et al., 2023)
Corn nitrogen use efficiency	The ability of corn to uptake applied nitrogen	(Mueller, et al., 2019)
Nitrogen Fertilizer	Application rate of nitrogen fertilizer per km <sup>2</sup> per year	(USDA, 2019)
Manure	Application rate of manure per km <sup>2</sup> per year	(Zhang, et al., 2017)
Atmospheric Nitrogen Deposition	Rate of deposition of atmospheric NO <sub>x</sub> and NH <sub>y</sub> .	(Vorosmarty, et al., 2023; Hegglin, et al., in preparation)
Extent of tile drainage	Percentage of cropland drained by tile drainage.	(Nakagaki, et al., 2016; Nakagaki & Wieczorek, 2016)
Precipitation	Depth of precipitation	(NLDAS, 2022; Xia, et al., 2012)
Temperature	Temperature	
Precipitation and Temperature extreme frequency	Derived from temperature and precipitation data using methods from (McKee, et al., 1993)	
Stream discharge	Rate of flow of water through river channels, modelled using the Water Balance Model.	(Vorosmarty, et al., 2023)

## Model Validation

Model outputs for the 2010s are validated with observations 1) at monitoring stations used for the original model calibration; and 2) at monitoring stations not used in the original model calibration. The model has an R<sup>2</sup> value of 0.887 and 0.894 for validations 1 and 2 respectively (see Figure S3)

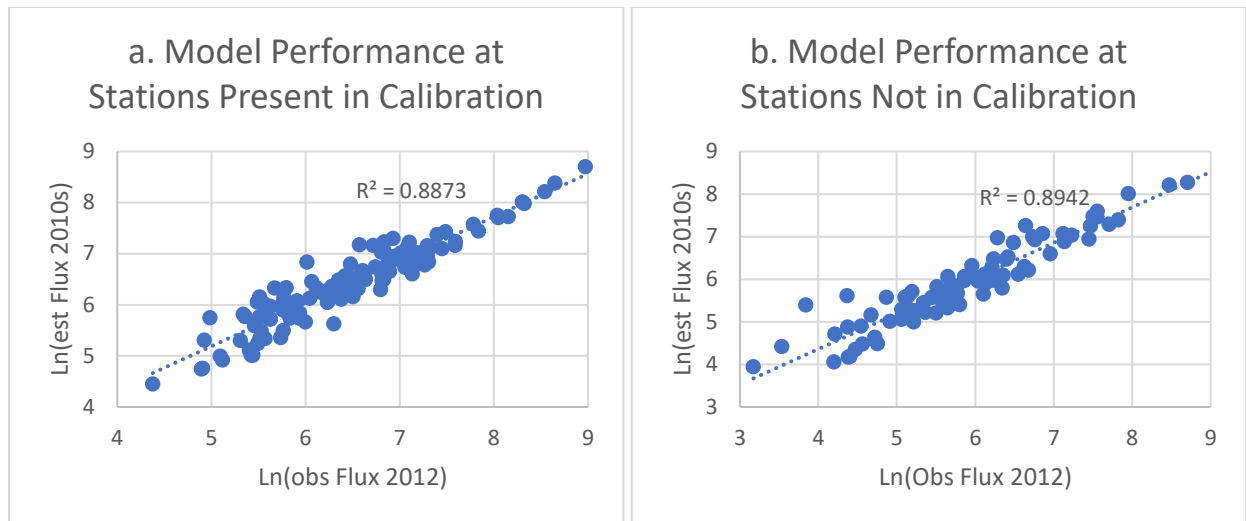


Figure S3 shows the agreement between log of simulated 2010s TN flux and log of observed 2012 TN flux

## References

Alexander, R. B. et al., 2008. Differences in Phosphorus and Nitrogen Delivery to the Gulf of Mexico from the Mississippi River Basin. *Environmental Science and Technology*, Volume 42, pp. 822-830.

Burke, A. et al., 2017. Risky Business: The impact of climate and climate variability on human population dynamics in western Europe during the last glacial maximum. *Quaternary Science Reviews*, Volume 164, pp. 217-229.

CIESIN, 2018. *Center for International Earth Science Information Network - CIESIN - SEDAC*. [Online] Available at: <https://sedac.ciesin.columbia.edu/data/set/gpw-v4-population-count-adjusted-to-2015-unwpp-country-totals-rev11> [Accessed 13 10 2022].

Hegglin, M. I., Kinnison, D., Lamarque, J. -F. & Al, E., in preparation. CCMI nitrogen deposition database (1850-2100) in support of CMIP6. *Geosci. Model Dev.*

Kicklighter, D. et al., this issue. Influence of forest infrastructure on the responses of ecosystem services to climate extremes in the Midwest and Northeast United States from 1980 to 2019. *Frontiers in Environmental Science*.

Maxfield, N. E. et al., 2021. *Investigating the Impact of Climate Extremes on Nitrogen Flux in CONUS Watersheds [POSTER]*. New Orleans, LA: s.n.

McKee, T. B., Doesken, N. J. & Kleist, J., 1993. The Relationship of Drought Frequency and Duration to Time Scales. *Proceedings of the 8th Conference on Applied Climatology*, 17(22), pp. 179-183.

Mueller, S. M., Messina, C. D. & Vyn, T. J., 2019. Simultaneous gains in grain yield and nitrogen efficiency over 70 years of maize genetic improvement. *Scientific Reports*, 9(9095).

Nakagaki, N. & Wieczorek, M. E., 2016. *Estimates of subsurface tile drainage extent for 12 Midwest states, 2012*, Reston, VA: US Geological Survey.

Nakagaki, N., Wieczorek, M. E. & Qi, S. L., 2016. *Estimates of subsurface tile drainage extent for the conterminous United States, early 1990s*, Reston, VA: US Geological Survey.

NLDAS, 2022. *North American Land Data Assimilation System (NLDAS)*. [Online]  
Available at: <https://ldas.gsfc.nasa.gov/nldas/nldas-get-data>  
[Accessed 13 10 2022].

Rychtecka, M. et al., n.d. Spatio-temporal Impact of Wastewater Point Sources on Nitrogen Pollution in U.S. Watersheds. *CUNY Thesis*.

Shih, J.-S. et al., 2022. Energy policy and coastal water quality: An integrated energy, air and water quality modeling approach. *Science of the Total Environment*, Volume 816, p. 151593.

Skinner, K. D. & Maupin, M. A., 2012. *Point-source nutrient loads to streams of the conterminous United States, 2012*, Reston, VA: US Geological Survey.

Smith, R. A., Schwarz, G. E. & Alexander, R. B., 1997. Regional interpretation of water-quality monitoring data. *Water Resources Research*, 33(12), pp. 2781-2798.

USDA, 2019. *Economic Research Service: Fertilizer Use and Price*. [Online]  
Available at: <https://www.ers.usda.gov/data-products/fertilizer-use-and-price.aspx>  
[Accessed 13 10 2022].

Vorosmarty, C. J. et al., this issue. A Framework to Study Climate-induced Extremes on the Food, Energy, Water Nexus and the Role of Engineered and Natural Infrastructure. *Frontiers*.

Xia, Y. et al., 2012. Continental-scale water and energy flux analysis and validation for the North American Land Data Assimilation System Project Phase 2 (NLDAS-2): 1. Intercomparison and application of model products. *Journal of Geophysical Research: Atmospheres*, 117(D3).

Zhang, B. et al., 2017. Global manure nitrogen production and application in cropland during 1860--2014: a 5 arcmin gridded global dataset for Earth system modeling. *Earth System Science Data*, 9(2), pp. 667-678.